

A vortex dynamics approach to the Nernst effect in fluctuating superconductors

S. Raghu¹, D. Podolsky², A. Vishwanath², and David A. Huse³

¹*Department of Physics, Stanford University, Stanford, CA 94305*

²*Department of Physics, University of California, Berkeley, CA 94720 and*

³*Department of Physics, Princeton University, Princeton, NJ 08544*

(Dated: January 17, 2008)

We present a new method to study the Nernst effect and diamagnetism of an extreme type-II superconductor dominated by phase fluctuations. We work directly with vortex variables and our method allows us to tune vortex parameters (e.g., core energy and number of vortex species). We find that diamagnetic response and transverse thermoelectric conductivity (α_{xy}) persist well above the Kosterlitz-Thouless transition temperature, and become more pronounced as the vortex core energy is increased. However, they *weaken* as the number of internal vortex states are increased. We find that α_{xy} closely tracks the magnetization ($-M/T$) over a wide range of parameters.

PACS numbers: 74.20.De, 74.25.Fy, 74.40+k, 74.72.-h

A number of experimental observations in superfluidity and superconductivity are best explained in terms of the statistical mechanics and dynamics of vortices. Examples include the Kosterlitz-Thouless (KT) transition in superfluid films, and the “flux-flow” contribution to electrical resistivity in type-II superconductors. A natural extension of this paradigm involves the use of thermoelectric and thermal transport experiments as a probe of vortex dynamics. This is especially pressing given the Nernst effect experiments in the cuprates [1]. The Nernst effect is defined as the appearance of a steady-state electric field (E_y) when a system is placed in a perpendicular thermal gradient ($\nabla_x T$) and magnetic field (H^z) under open circuit conditions. In the cuprate superconductors, a large Nernst signal and diamagnetic response persists well above T_c , the superconducting transition temperature, and are especially enhanced in the underdoped regime of hole-doped materials.

To explain these results, it has been argued that vortices are responsible for the large Nernst signal [1]: as a vortex drifts down the temperature gradient, it generates a transverse electric field. A vortex description above T_c is useful when the superconducting transition represents the loss of macroscopic phase coherence, while the amplitude of the order parameter remains large below a higher ‘mean-field’ temperature scale $T_c^{MF} \gg T_c$ [2]. This idea is most likely to hold true in the underdoped regime of the hole-doped cuprates, where the reduced superfluid stiffness enables phase fluctuations to suppress T_c well below the mean-field transition temperature. This “vortex-liquid regime” regime $T_c < T \ll T_c^{MF}$ [3] over a range of fields can be intuitively understood in terms of a dilute fluid of vortices, but so far this appealing picture [4, 5] has not lead to a quantitative understanding of the Nernst effect.

There are special challenges involved in constructing a vortex based theory of thermoelectric transport that is consistent with the basic principles of statistical mechanics. In contrast to thermodynamics, and even electrical

transport, where a theory of vortices interacting via a long range potential can be used, a thermal or Nernst transport calculation requires a purely local formulation where no such long range forces are explicitly present. In this Letter, we present such a local formulation, and use it to study thermoelectric transport directly in the vortex language. An advantage of our method is that vortex parameters such as core energy, or number of vortex species, can be tuned independently of other properties, and their impact on the Nernst signal and magnetization can be systematically studied. Moreover, it is possible to use our method to study the Coulomb gas efficiently even in the high density limit, where the number of pairwise Coulomb interactions is large.

Previous theoretical work on the Nernst effect in cuprates [6, 7, 8, 9, 10] has studied the time-dependent Ginzburg-Landau theory, which includes fluctuations in the amplitude of the order parameter. In earlier work, three of us have studied the Nernst effect in an XY model [11], which should be relevant for the underdoped cuprates. Our present results approaching from the vortex viewpoint are consistent with this earlier approach. Remarkably, we find that the close quantitative connection between the Nernst effect and diamagnetism observed in that and other papers, holds in the present study too, even when vortex properties are drastically modified.

Method: Consider a two dimensional superconductor in the extreme type-II limit, in which the supercurrents are too feeble to modify the externally imposed field. Since we are interested in the ‘vortex liquid’ regime, we restrict the order parameter to live on the sites n of a square lattice and assume that all fluctuations arise from the phase: $\psi_n(t) = |\psi_0|e^{i\theta_n(t)}$. We map to the vortex representation by defining a *dual* electric field $\mathbf{e} = (e_i^x, e_i^y)$ on the bonds $(i, i + \hat{x})$; $(i, i + \hat{y})$ of a dual lattice, orthogonal to the original lattice bonds, via: $\mathbf{e} = \nabla\theta \times \hat{\mathbf{z}}$ where ∇ is a lattice derivative. The local field \mathbf{e} is related to the local supercurrents via $\mathbf{J} = \rho_s^0 \hat{\mathbf{z}} \times \mathbf{e}$, where ρ_s^0 is the

bare superfluid density. Vortices may live at the sites i of this dual lattice, and the integer vortex charge n_i satisfies Gauss' law $\nabla \cdot \mathbf{e} = 2\pi n_i$. We thus obtain a completely local Hamiltonian for the vortex fluid that retains all phase and vortex degrees of freedom:

$$\mathcal{H} = \frac{1}{4\pi} \sum_i \mathbf{e}_i^2 + \epsilon_c \sum_i n_i^2, \quad (1)$$

where ϵ_c is the vortex core-energy and we use units where $\rho_s^0 = 1/2\pi$. When the transverse electric fields are integrated out, the model reduces to the static 2D Coulomb gas. However, we stress that one must include both local supercurrents and vortices when dealing with thermal transport, so as to define a local energy density. The interaction between the vortices is mediated by the supercurrents, and this maps simply to the interaction between the charges being mediated by the dual electric field in the Coulomb gas.

The model is given a Monte Carlo dynamics that captures the effect of random thermal fluctuations. Two distinct types of updates, charge and curl updates, corresponding to the two degrees of freedom (vortices and supercurrents) are introduced (Fig. 1). During a curl update, a plaquette is chosen at random and a random electric curl is added to it. Such an electric flux configuration is purely transverse and is not accompanied by vortex creation. During a charge update, a lattice bond is chosen at random, and a vortex/anti-vortex pair is added on the two sites connected to this bond. The electric fluxes are updated locally near the charges to satisfy Gauss' law. Note, this charge update may result in the motion a pre-existing vortex. In the simulation, each move is accepted with probability $1/[1 + \exp(\Delta U/T)]$, where ΔU is the change in energy associated with the move and T is the local temperature at the center of the plaquette or bond for that move. By varying the relative frequency of each type of trial, we have control over D_{ph} , the phase diffusivity, relative to the vortex diffusivity D_v . In what follows, we work in the physically reasonable limit $D_{ph} \gg D_v$. After an attempt is made to update each bond and plaquette with such moves, a unit of Monte Carlo time passes in the simulation. A related method (without pair creation) has been used in Ref. [12, 13] to study charged polymers.

When a charge move is attempted, the simplest way to satisfy Gauss' law is to add an electric flux $\mathbf{e} = 2\pi\hat{\mathbf{r}}$ to the link $\hat{\mathbf{r}}$ connecting the positive to the negative charge. However, such single bond updates usually produce large ΔU and thus are rarely accepted, resulting in too little vortex motion at low temperatures; hence an update that spreads the electric flux over several bonds is used. A simple example of such an update is shown in Fig. 1. The added flux is made curl-free and the move we actually use involves a patch of 12 plaquettes that is one plaquette larger in all directions than indicated in Fig. 1.

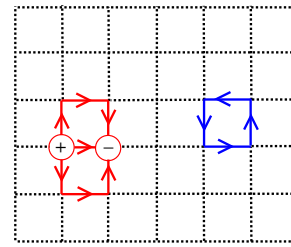


FIG. 1: Charge updates (left) and curl updates (right) sample the longitudinal and transverse degrees of freedom, respectively, of the dual electric field.

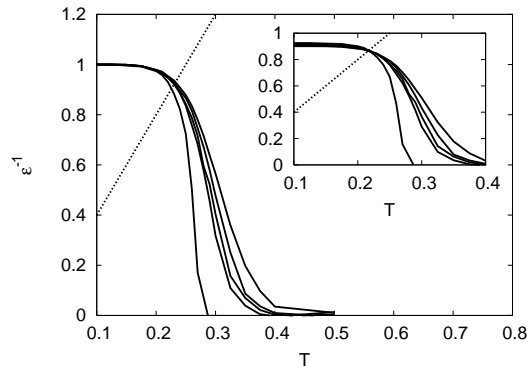


FIG. 2: Dielectric response of the dual Coulomb gas, computed using Eq. 2, and (inset) rescaled for finite-size effects [14]. We use an $L \times L$ torus with $L = 8, 10, 12, 14, 40$, and core energy $\epsilon_c = 0.125$. The transition temperature is the location where the rescaled data intersects the line $y = 4T$ (dotted line).

Thermodynamics: We have studied the KT transition of the neutral 2D Coulomb gas by tracking the dielectric response function

$$\epsilon^{-1} = 1 - \frac{\langle (\sum_i \mathbf{e}_i)^2 \rangle}{4\pi T L^2}. \quad (2)$$

At $T = T_{KT}$, the dielectric response function satisfies the universal jump criterion [15]:

$$\epsilon^{-1} = \begin{cases} 4T_{KT}, & T = T_{KT}^- \\ 0, & T = T_{KT}^+ \end{cases} \quad (3)$$

Fig. 2 shows the results of the helicity modulus calculation using various system sizes and a core energy $\epsilon_c = 0.125$. We use finite-size scaling [14] to identify $T_{KT} = 0.22$; the naive free-energy estimate is $T_{KT}^0 = 0.25$ in our units. In the remainder of this letter, we cite all temperatures in units of T_{KT}^0 .

Diamagnetism: When a magnetic field is applied, the resulting imbalance of vorticity leads us to consider a plasma of vortices in a static, neutralizing background (charge density $n_b = -B/\Phi_0$), where $\Phi_0 = 2\pi$ is the flux quantum in our units. To study diamagnetism we must permit vortices to enter and leave the sample, so we em-

ploy a cylindrical geometry with open boundaries. Current flow near the boundaries is measured, which arises due to a surface depletion of vorticity. This has a lower free energy than the perfectly neutral system, and leads to diamagnetism. Deep inside the cylinder, beyond some distance x_0 from the edge, the supercurrents vanish in equilibrium. The magnetization can be obtained by inverting the relation $\mathbf{J} = \nabla \times \mathbf{M}$ on a cylinder whose axis is along the x direction. For physical clarity we present continuum formulas below, these can be readily transcribed into the appropriate lattice versions. We have:

$$M = \int_0^{x_0} dx \langle J^y(x, y) \rangle = \rho_s \int_0^{x_0} dx \langle e_x \rangle. \quad (4)$$

Thus, the magnetization is directly proportional to the *work function* of the dual Coulomb gas (energy cost of removing a vortex from the bulk of the system). Using Gauss' law we can also obtain:

$$M = 2\pi\rho_s \int_0^{x_0} dx x (\langle n(x) \rangle - B/\Phi_0). \quad (5)$$

Thus, the magnetization is also the total edge polarization (dipole moment) per unit length. The polarization fields are non-zero only in the charge depletion region near the cylinder's edge.

Nernst Effect: To determine the Nernst effect, we again make use of cylindrical geometry, and apply a temperature gradient along the cylinder axis. In our simulations, we compute the transverse thermoelectric conductivity α_{xy} defined via $\langle J_y \rangle = -\alpha_{xy}(-\nabla_x T)$. The thermoelectric conductivity is closely related to the Nernst signal: α_{xy}/σ_{xx} , where σ_{xx} is the electrical conductivity and we have made the approximation of vanishing Hall angle. In our calculations, α_{xy} is obtained by measuring the dual electric field e^x , and using the relation $\alpha_{xy} = \langle e^x \rangle / \nabla_x T$. Thus while α_{xy} is an off-diagonal transport coefficient when written in terms of electrical currents, it is a *diagonal* response function in the vortex representation: it is simply the vortex *thermopower*. We have verified that the net vortex motion vanishes once the steady-state in the thermal gradient is reached, as is required in a thermopower measurement. The quantity α_{xy} has the advantage that, unlike the Nernst signal e_N , it does not have any explicit dependence on t_{mc} , the Monte-Carlo time step, as can be seen from the Kubo formula for α_{xy} and from dimensional analysis [11].

Figure 3 shows the simulation results for α_{xy} and M (inset b) for applied fields up to $B_0 = \Phi_0/(2\pi a^2)$, where a is the lattice spacing, comparable to the zero temperature coherence length ξ_0 . Both α_{xy} and $-M/T$ are expressed in units of the 2D ‘‘quantum of thermoelectric conductance,’’ $2ek_B/h$. We show data for $T \geq T_{KT}^0$; below T_{KT}^0 , our simulations encounter difficulties due to impaired vortex mobility, and furthermore, it is difficult to apply

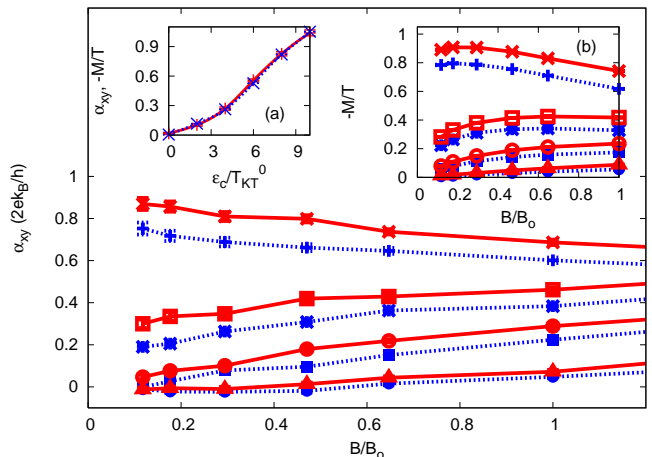


FIG. 3: α_{xy} for a system of single-flavor (solid lines) and 2-flavor (dotted lines) vortices on a 20×15 cylinder, with core energy $\epsilon_c = 0.5T_{KT}^0$. Temperatures shown are 1.0 (topmost 2 curves), 1.25, 1.5, and 2.0 T_{KT}^0 (bottom 2 curves). *Inset a:* Core energy dependence of α_{xy} (solid lines) and $-M/T$ (dashed lines) in units of $2ek_B/h$ for single-flavor vortices, at $T = 2.5T_{KT}^0$, $B = 0.7B_0$ showing a marked increase of both quantities with core energy. *Inset b:* Diamagnetism $-M/T$ curves for the same temperatures as the main figure. (Units of $2ek_B/h$ are used on the vertical axes of both insets.)

thermal gradients small enough to remain within linear response. Fortunately, $T \geq T_{KT}^0$ is a regime of interest, since the Nernst signal persists well above T_c in the experiments of Wang, *et al.* [1]. The results presented here are in quantitative agreement with earlier computations involving the 2D XY model with Langevin dynamics [11]: in particular, both models have the feature that in the small magnetic field limit, a) α_{xy} and M diverge logarithmically as $B \rightarrow 0$ for $T \leq T_{KT}$ and b) they increase linearly with B at small B when $T > T_{KT}$ [16]. Similar features have been seen in experiments of Wang, *et al.* [1]. Moreover, both α_{xy} and M are detectable at temperatures as high as $2T_{KT}$ in this vortex model, which is also consistent with 2D XY model results [11]. At very high temperatures $T \gg T_{KT}$, the 2D XY model predicts that α_{xy} and M/T decay sharply as a power law in temperature. In the vortex model, however, the magnetization decreases even more rapidly at such high temperatures: a calculation based on the dual solid-on-solid model, shows that the magnetization of single-flavor vortices decays exponentially as: $M = -2T \sin(B/B_0) e^{-2T/\rho_s}$. We have checked that our numerical results agree with this expression. Although we have not succeeded in finding similar expressions for α_{xy} , our numerical results indicate that α_{xy} also decays in this fashion at high temperatures and closely tracks the diamagnetism.

Vortex Core Energy Dependence: The core energy dependence of α_{xy} and diamagnetism $-M/T$ are shown in Fig. 3 (inset a) at $T = 2.5T_{KT}^0$. So long as $\epsilon_c \gg T$,

both are found to increase with ϵ_c . At this temperature, α_{xy} and $-M/T$ track each other closely. With increasing core energy, α_{xy} and $-M/T$ rise from near zero at $\epsilon_c = 0$ to $O(1)$ at $\epsilon_c = 10T_{KT}^0$, showing that the core energy has a dramatic impact on both of these quantities in this regime. The dominant effect of the vortex core energy ϵ_c is that it enhances local superconducting correlations at short distances by increasing the cost of vortex fluctuations. The core energy enters directly in setting the “work function” for removing a vortex from the system, which is proportional to the magnetization. For $\epsilon_c \gg T$, we thus expect $-M \propto \epsilon_c$, since more vortices are expelled near the boundaries in this limit. We have observed this in our simulations. The vortex-free boundary layer grows with ϵ_c and when it becomes comparable to the thickness of the sample this causes strong finite-size effects. Thus we have not been able to reliably determine the bulk behavior for large values of the vortex core energy ϵ_c . We expect α_{xy} to saturate at a finite value in this limit – when all thermally-generated vortex fluctuations are suppressed, the remaining field-induced vortices respond to the thermal gradient in a way that is independent of the magnitude of ϵ_c . We do see indications of the saturation of α_{xy} at large values of ϵ_c , although we have not been able to access this regime reliably due to the large finite-size effects on α_{xy} when $\epsilon_c \gg T$.

Dependence on the Number of Vortex Flavors: Several theories of cuprates predict additional degrees of freedom associated with vortices, that endows them with a flavor index [17, 18]. Such an extension is readily incorporated in our formalism, the Gauss law is now $\nabla \cdot \mathbf{e} = 2\pi \sum_{\alpha=1}^{N_v} n_{i\alpha}$ where α is the flavor index. Our data shows a systematic dependence on the number of internal flavors of vortices. We find that both $|M|$ and α_{xy} of single-flavor vortices (solid curves in Fig. 3) are systematically larger than that of vortices with 2 internal flavors (dotted lines). With multiple vortex species, there is additional configurational entropy associated with the internal degree of freedom. Therefore, the free energy cost of introducing a vortex into the sample is lower, and the system becomes less diamagnetic. It is more difficult to understand, however, why α_{xy} decreases as the number of species is increased. In phenomenological discussions, the transport coefficient α_{xy} is usually identified with the vortex entropy [19]. Therefore, one may naively expect α_{xy} to increase with the number of internal vortex flavors. Moreover, α_{xy} is equivalent to the vortex thermopower, and if we neglected the logarithmic interactions between vortices, a simple calculation shows that the thermopower of an ideal gas of vortices is simply the entropy per particle [20]; which increases linearly with the number of internal states associated with such particles. Our numerical results however are in sharp contrast to such expectations that α_{xy} ought to be proportional to an effective entropy per vortex. Instead, our

results which have the opposite trend point towards a scenario that is far more complicated than an ideal gas approximation; interactions between vortices and thermally generated vortex-antivortex pairs invalidate such simple relations between α_{xy} and vortex entropy.

Perhaps the most striking feature of our data is the fact that α_{xy} and $-M/T$ closely track each other. In particular, at high temperatures, our results obey the relation $\alpha_{xy} = -cM/T$, where $c \approx 1$, and is difficult to determine accurately due to noise at large temperatures. Recently, it was shown analytically in Ref. [11] that for the 2D XY Hamiltonian with overdamped dynamics, $c = 1/2$ at high temperatures. Furthermore, one obtains the same relation for Gaussian superconducting fluctuations [21]. Here, we have shown that this relation is even more robust, since it hardly depends on the variation of the core energy and the number of distinct vortex species so long as ϵ_c is not much greater than T . This relationship which connects a transport coefficient and a thermodynamic quantity is indicative of a deep underlying (and as yet unknown) principle, that seems to hold true over a broad range of parameters.

In conclusion, we have presented a new local method to study the thermodynamic and transport properties of 2D vortex liquids. This method enables us to directly observe the effect of tuning vortex parameters on α_{xy} and M . As an application of our method, we have systematically studied the effect of modifying the vortex core energy and the number of vortex species on diamagnetism and Nernst effect. In all cases, we have found that both quantities persist well above T_{KT} and α_{xy} closely tracks $-M/T$ when $T_{KT} < T \ll \epsilon_c$. We have provided the first detailed analysis of the Nernst effect of a vortex liquid that deals directly with vortex variables. The method presented here can be generalized to study thermal transport of vortex liquids in 3D, and can be extended to study quantum phase fluctuations at low temperatures.

We thank P. W. Anderson, P.A. Lee and N. P. Ong for very helpful discussions. This work was supported by NSF DMR-0645691 (A. V.), -0213706 (D.A.H.) and by the Stanford Institute for Theoretical Physics (S. R.).

-
- [1] Y. Wang, L. Li, and N. P. Ong, Phys. Rev. B **73**, 024510 (2006).
 - [2] V. J. Emery and S. A. Kivelson, Nature **374**, 434 (1995).
 - [3] D. S. Fisher, M. P. A. Fisher, and D. A. Huse, Phys. Rev. B **43**, 130 (1991).
 - [4] L. B. Ioffe and A. J. Millis, Phys. Rev. B **66**, 094513 (2002).
 - [5] C. Honerkamp and P. A. Lee, Phys. Rev. Lett. **92**, 177002 (2004).
 - [6] I. Ussishkin, S. L. Sondhi, and D. A. Huse, Phys. Rev. Lett. **89**, 287001 (2002).
 - [7] S. Mukerjee and D. A. Huse, Phys. Rev. B **70**, 014506 (2004).

- [8] P. W. Anderson, arXiv:cond-mat/0603276.
- [9] P. W. Anderson, Nature Physics **3**, 160 (2007).
- [10] S. A. Hartnoll, P. K. Kovtun, M. Mueller, and S. Sachdev, Phys. Rev. B **76**, 144502 (2007).
- [11] D. Podolsky, S. Raghu, and A. Vishwanath, Phys. Rev. Lett. **99**, 117004 (2007).
- [12] A. C. Maggs and V. Rossetto, Phys. Rev. Lett. **88**, 196402 (2002).
- [13] L. Levrel and A. C. Maggs, Phys. Rev. E **72**, 016715 (2005).
- [14] H. Weber and P. Minnhagen, Phys. Rev. B **37**, 5986 (1988).
- [15] D. R. Nelson and J. M. Kosterlitz, Phys. Rev. Lett. **39**, 1201 (1977).
- [16] V. Oganesyan, D. A. Huse, and S. L. Sondhi, Phys. Rev. B **73**, 094503 (2006).
- [17] P. A. Lee and X.-G. Wen, Phys. Rev. B **63**, 224517 (2001).
- [18] D. P. Arovas, A. J. Berlinsky, C. Kallin, and S.-C. Zhang, Phys. Rev. Lett. **79**, 2871 (1997).
- [19] C. Caroli and K. Maki, Phys. Rev. **164**, 591 (1967).
- [20] S. Raghu, D. Podolsky, and A. Vishwanath, to be published.
- [21] I. Ussishkin, unpublished.